Supplementary Information (SI) for CrystEngComm.
This journal is © The Royal Society of Chemistry 2025

A dynamic pcu MOF(Zn) containing a ditopic T-shaped [2]rotaxane linker

Hazem Amarne,[a] Alexander J. Stirk [b], Christopher A. O'Keefe[b], Robert W. Schurko[c,d] and Stephen J. Loeb*[b]

a. *Department of Chemistry, The University of Jordan, Amman, 11942, Jordan*
b. *Department of Chemistry and Biochemistry, University of Windsor, Windsor, ON, Canada N9B 3P4.*
c. *Department of Chemistry and Biochemistry, Florida State University, Tallahassee, FL, 32306 USA*
d. *National High Magnetic Field Laboratory, Tallahassee, FL 32310*

Table of Contents

1. Materials and General Procedures

All solvents were purchased from Sigma-Aldrich, $HBF_4.Et_2O$, $ZrCl_4$, $Zn(NO_3)_2.6H_2O$, 3,5-dimethoxybenzaldehyde, and 2,1,3-benzothiadiazole, were purchased form Sigma-Aldrich, pentaethylene glycol and 5-bromopentene were purchased from TCI Chemicals, concentrated nitric acid was purchased from Fisher Scientific, and 4-carboxylphenylboronic acid pinacol ester was purchased from Frontier Scientific. All purchased reagents were used without further purification. Deuterated solvents for NMR ($CDCl_3$, CD_3CN, DMSO-d_6) were purchased from Cambridge Isotope Laboratories. Thermal gravimetric analyses (TGA) on the metal-organic frameworks were conducted on a Mettler Toledo SDTA 851e instrument. Samples were normalised for 30 min at 25 °C before heating at 5 °C min^{-1} to a maximum of 550 °C. Solution NMR experiments for ^1H and ^{13}C nuclei were conducted on either a 300 MHz or 500 MHz Bruker Advance instrument at room temperature – frequencies for different nuclei are reported below for each individual molecule. Each solution NMR is reported in ppm relative to tetramethylsilane (TMS, $Si(CH_3)_4$), with the individual solvent signal as the reference peak. Mass spectrometry data was conducted on a Waters Xevo GS-XS ToF instrument in either ASAP+ or ESI+ mode. Pentaethyleneglycol-dipent-4-enyl ether,[1] 4,7-dibromo-2,1,3-benzothiadiazole,[2-4] 3,6-dibromo-1,2-benzenediamine,[4,5] and 4,7-dibromo-2-(3,5-dimethoxyphenyl)-1H-benzo[d]imidazole[6] were synthesized based on previously reported procedures.

2. Synthesis of Ligands and MOFs

Synthesis of Diester Axle 2

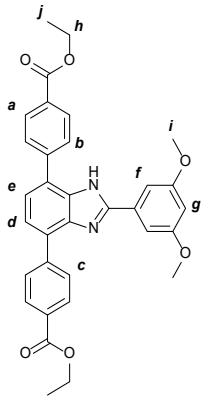

4,7-Dibromo-2-(3,5-dimethoxyphenyl)-1H-benzo[d]imidazole, **1** (1.70 g, 4.12 mmol), (4-(ethoxycarbonyl)phenyl)boronic pinacol ester (2.00 g, 10.31 mmol) and K_2CO_3 (2.85 g, 20.62 mmol) were added to a Schlenk flask, evacuated and back-filled with N_2. $[Pd(PPh_3)_4]$ (0.24 g, 5 mol%) was then added to the flask under N_2. Degassed THF/H_2O (1:1, 80 mL) was transferred to the flask *via* a cannula. The flask was then purged with N_2 and reacted at 75 °C for 24 h. Reaction was monitored by TLC using EtOAc/hexanes (1:1) as the mobile phase. When no spot was observed for the (4-(ethoxycarbonyl)phenyl) boronic pinacol ester on the TLC, the reaction was cooled to room temperature. The spot observed for the product was found to have an R_f of 0.49. Upon cooling, an interface formed; additional THF was added and separated from the aqueous phase. The aqueous phase was washed twice with THF, with the organic layers being combined and evaporated to dryness. The solid was then dissolved in DCM and washed with saturated, aqueous NaCl solution. The organic layer was finally dried on anhydrous $MgSO_4$ and evaporated. Purification was done by suspending the yellow solid in anhydrous EtOH, boiling and cooling to room temperature. Upon filtering an off-white solid was observed. After dissolving the solid in DCM and filtering through Celite and a subsequent evaporation, the pure white compound was isolated. Yield 1.60 g, 70%. M.P.: 231 °C.

^{1}H NMR (500 MHz, $CDCl_3$): δ = 10.32 *NH* (s, 1H), 8.10 *a* (d, J = 7.8 Hz, 4H), 7.95 *b,c* (s, 4H), 7.45 *d,e* (s, 2H), 7.32 *f* (d, J = 2.3 Hz, 2H), 6.55 *g* (t, J = 2.3 Hz, 1H), 4.38 *h* (q, J = 7.1 Hz, 4H), 3.83 *i* (s, 6H), 1.42 *j* (t, J = 7.1 Hz, 6H).

^{13}C NMR (125 MHz, $CDCl_3$): δ = 166.72, 161.33, 152.53, 142.83, 131.50, 130.14, 129.47, 128.71, 123.14, 105.29, 102.63, 61.24, 55.75, 53.56, 14.48.

HR-MS (ToF ASAP+): Calculated for $[M+H]^+$: $[C_{33}H_{31}N_2O_6]^+$ m/z = 551.2100; found m/z = 551.2181.

Synthesis of Axle Linker 3

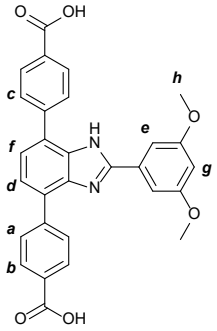

The diester **2** (144 mg, 0.262 mmol) was dissolved in EtOH/THF (10 mL, 1:1 v/v) and NaOH (5 mL, 2 mol L^{-1}) added. The mixture was heated at reflux for 12 h, turning the solution yellow. After cooling to room temperature, the organic solvents were evaporated off. Additional distilled water was added to the solution and then acidified to pH 4 by adding HCl (1 mol L^{-1}) dropwise. At pH 4, a yellow precipitate was observed and a yellow solution observed. The mixture was then centrifuged several times, whilst decanting excess water. The solid was then filtered through a PTFE filter, washed with distilled water and air dried yielding a red/brown solid. Yield 70 mg, 79%. M.P.: ~328 °C (dec.).

^{1}H NMR (500 MHz, DMSO-d_6) δ = 12.72 *NH* (s, 1H), 8.36 *a* (d, J = 8.0 Hz, 2H), 8.13 *b* (t, J = 9.0 Hz, 4H), 7.88 *c* (d, J = 7.6 Hz, 2H), 7.64 *d* (s, 1H), 7.51 *e* (d, J = 2.2 Hz, 2H), 7.41 *f* (s, 1H), 6.66 *g* (t, J = 2.3 Hz, 1H), 3.84 *h* (s, 6H).

^{13}C NMR (125 MHz, DMSO-d_6) δ = 167.33, 160.70, 152.76, 142.25, 141.98, 133.53, 131.66, 129.95, 129.43, 129.10, 128.97, 128.79, 125.13, 123.63, 121.74, 105.62, 101.97, 55.58.

HR-MS (ToF ESI+): Calculated for $[M+H]^+$: $[C_{29}H_{22}N_2O_6]^+$ m/z = 495.1500; found m/z = 495.1556.

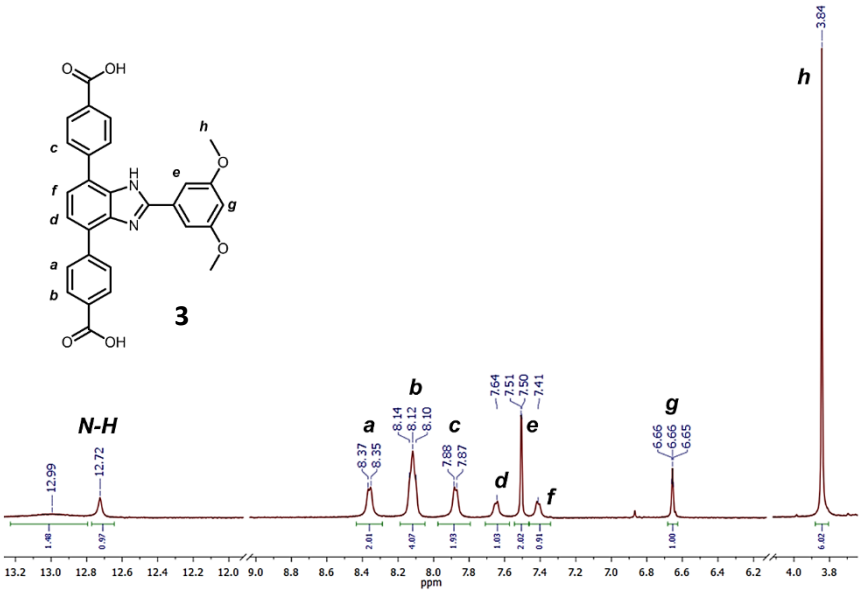

Figure S1. ^{1}H NMR (500 MHz, DMSO-d_6) of axle linker **3**.

Formation of [H-2][BF_4]

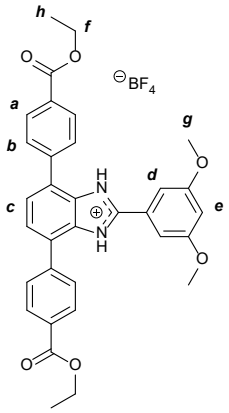

The diester **2** (1.5 g, 3.64 mmol), was suspended in MeCN (40 mL) and sonicated. To this suspension $HBF_4.Et_2O$ (1.1 eq) was added carefully. The mixture turned a slight orange colour and the suspension sonicated until a clear solution was achieved. The solution was filtered, and the solution evaporated to dryness. Et_2O was added (10 mL) revealing a white precipitate. The precipitate was filtered off as pure compound and used in the next step without further purification. Yield 2.10 g, 90%. M.P.: >235 °C (dec.).

^{1}H NMR (500 MHz, CD_3CN) δ = 12.28 *NH* (s, 2H), 8.23 *a* (d, J = 7.9 Hz, 4H), 7.85 *b* (d, J = 8.0 Hz, 4H), 7.76 *c* (s, 2H), 7.16 *d* (d, J = 2.2 Hz, 2H), 6.86 *e* (t, J = 2.3 Hz, 1H), 4.41 *f* (q, J = 7.1 Hz, 4H), 3.88 *g* (s, 6H), 1.41 *h* (t, J = 7.1 Hz, 6H).

^{13}C NMR (125 MHz, CD_3CN) δ = 167.08, 162.50, 152.64, 140.68, 131.94, 131.22, 130.86, 130.23, 128.49, 128.37, 124.27, 108.28, 107.11, 62.35, 56.81, 14.63.

Synthesis of [2]Rotaxane Diester [H-4][BF_4]

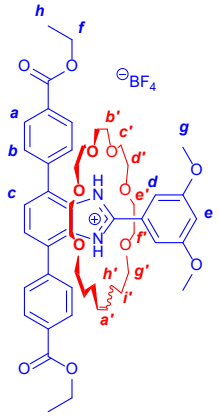

[H-**2**][BF_4] (1.20 g, 1.80 mmol) and pentaethyleneglycol-dipent-4-enyl ether (0.85 g, 2.27 mmol) were added to a Schlenk flask and dissolved in dry, degassed DCM (100 mL) and stirred under N_2 until a clear, brown solution was observed. The flask was evacuated and backfilled with N_2 several times. Grubbs Catalyst Gen. I (0.16 g, 10 mol%) was added under N_2 to the reaction flask. The flask and reflux condenser were evacuated and backfilled with N_2 three times to ensure an inert environment. The reaction was then heated at 40 °C, with aliquots taken every 12 h to observe reaction progress. Additional portions of 5 mol% of Grubbs Catalyst were added every 12 h. After 3 d, no more alkene peaks associated with the pentaethyleneglycol-dipent-4-enyl ether were observed, and the reaction quenched with ethoxy ethylene (1 mL). The solvents were then removed by evaporation. The residue was dissolved in EtOAc and washed with saturated $NaHCO_3$ (*aq*) three times and once with NaCl(*aq*) solution. The organic layers were collected and dried on anhydrous $MgSO_4$. After concentrating the organic solution, the mixture was purified on a silica column using hexanes/EtOAc (1:2) with NEt_3 (1%). Two fractions containing each isomer of the product were found with R_f values of 0.53 and 0.47. Since the next step results in hydrogenation of all alkene double bonds, the E/Z isomer fractions were combined. Yield 1.00 g, 54%. M.P.: ~256 °C (dec.). For the subsequent synthesis and ease of further characterisation the product was acidified using $HBF_4.Et_2O$ (1.1 eq). M.P.: ~240 °C (dec.).

^{1}H NMR (500 MHz, CD_3CN, HBF_4 salt): δ = 13.21 *NH* (s, 2H), 8.22 *a* (d, J = 8.4 Hz, 4H), 7.91 *b* (d, J = 8.4 Hz, 4H), 7.79 *c* (s, 2H), 7.55 *d* (d, J = 2.3 Hz, 2H), 6.87 *e* (t, J = 2.2 Hz, 1H), 5.07 *a'* (t, J = 3.8 Hz, 2H), 4.40 *f* (q, J = 7.1 Hz, 4H), 3.85 *g* (s, 6H), 3.44 – 2.61 *b', c', d', e', f', g'* (m, 24H), 1.87 – 1.78 *h'* (m, 4H), 1.50 – 1.43 *i'* (m, 4H), 1.40 *h* (t, J = 7.1 Hz, 6H).

^{13}C NMR (125 MHz, CD_3CN, HBF_4 salt): δ = 166.74, 161.94, 153.04, 140.95, 132.02, 131.09, 130.97, 130.81, 130.68, 130.56, 129.79, 128.80, 125.98, 110.45, 109.76, 106.77, 106.10, 72.70, 71.33, 71.21, 71.10, 70.91, 70.71, 70.62, 70.55, 70.14, 62.21, 56.92, 49.90, 31.29, 30.20, 28.97, 25.69, 14.60.

HR-MS (ToF ESI+): Calculated for $[M+H]^+$: $[C_{51}H_{65}N_2O_{12}]^+$ m/z = 897.4500; found m/z = 897.4537.

Synthesis of Rotaxane Diester 5-d_2

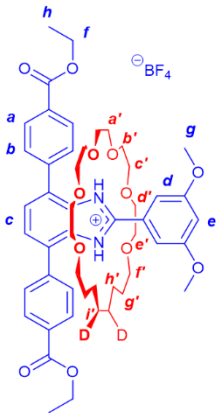

[H-**5**][BF_4]-d_2

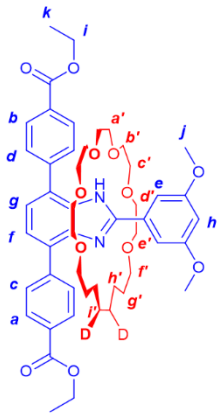

5-d_2

[H-**4**][BF_4] (1.00 g, 1.00 mmol) was added to a Schlenk flask and dissolved in MeOH (80 mL). The flask was then evacuated and backfilled with N_2. Pd/C (11 mg, 10 wt%) was added under N_2. The flask was placed under vacuum again, with D_2 added to the flask, with stirring, *via* a balloon. The mixture was reacted at room temperature for 4 h, with aliquots taken each hour to monitor the disappearance of the alkene peak. After no more alkene peaks were present in the ^{1}H NMR spectrum, the reaction was flushed with N_2. The solution was filtered over Celite, removing Pd/C. The solution was evaporated to dryness, leaving a white crystalline solid which was used in further synthesis without additional purification. Yield of [H-**5**][BF_4]-d_2 0.85 g, 84%. M.P.: ~ 243 °C (dec).

^{1}H NMR (500 MHz, CD_3CN, HBF_4 Salt): δ = 13.11 *NH* (s, 2H), 8.23 a(d, J = 8.3 Hz, 4H), 7.88 b(d, J = 8.4 Hz, 4H), 7.83 c(s, 2H), 7.49 d(d, J = 2.3 Hz, 2H), 6.86 e(t, J = 2.3 Hz, 1H), 4.40 f(q, J = 7.1 Hz, 4H), 3.83 g(s, 6H), 3.45 – 2.66 a', b', c', d', e', f'(m, 24H), 1.41 h(t, J = 7.1 Hz, 6H), 1.22 – 0.75 g', h', i'(m, 10H).

^{13}C NMR (125 MHz, CD_3CN, HBF_4 Salt): δ = 166.72, 161.93, 152.82, 140.87, 131.96, 131.05, 130.55, 129.98, 128.68, 128.58, 126.15, 106.60, 72.73, 71.25, 71.21, 71.08, 70.70, 70.58, 62.19, 56.86, 30.22, 27.97, 27.83, 27.71, 25.35, 14.57.

To characterise the neutral compound, [H-**5**][BF_4]-d_2 (30 mg, 0.03 mmol) was suspended in EtOAc (10 mL) and NEt_3 (~1 eq) was added drop wise with sonication until a clear solution formed. The organic solution was then washed once with distilled water and once with saturated NaCl(*aq*) solution. The organic washings were then dried on Na_2SO_4 and evaporated. Yield of **5**-d_2 24 mg, 80%. M.P: 183 °C.

^{1}H NMR (500 MHz, CD_2Cl): δ = 11.93 N-H(s, 1H), 8.20 a(d, J = 8.1 Hz, 2H), 8.16 b(d, J = 8.4 Hz, 2H), 8.11 c(d, J = 8.4 Hz, 2H), 7.83 d(d, J = 8.4 Hz, 2H), 7.80 e(d, J = 2.3 Hz, 2H), 7.51 f(d, J = 7.7 Hz, 1H), 7.34 g(d, J = 7.7 Hz, 1H), 6.52 h(t, J = 2.3 Hz, 1H), 4.40 i(qd, J = 7.1, 1.9 Hz, 4H), 3.85 j(s, 6H), 3.29 – 2.94 a', b', c', d', e'(m, 22H), 2.88 – 2.81 f'(m, 2H), 1.42 k(td, J = 7.1, 2.2 Hz, 6H), 1.35 – 1.21 g', h'(dt, J = 13.5, 7.1 Hz, 8H), 0.95 – 0.87 i'(m, 2H).

^{13}C NMR (125 MHz, CD_2Cl_2): δ = 166.95, 166.65, 160.41, 155.59, 144.36, 144.21, 143.10, 133.47, 131.39, 130.19, 129.98, 129.69, 129.21, 125.46, 123.45, 121.86, 110.15, 103.28, 71.57, 70.57, 70.33, 69.87, 69.61, 69.32, 61.45, 61.21, 56.36, 46.63, 29.89, 26.14, 14.56.

HR-MS (ToF ES+): Calculated for $[M+H]^+$: $[C_{51}H_{65}D_2N_2O_{12}]^+$ m/z = 901.4700; found m/z = 901.4806.

Synthesis of [2]Rotaxane Linker 6-d_2

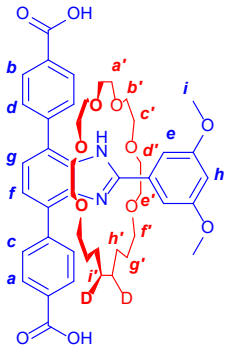

[H-**5**][BF_4]-d_2 (0.80 g, 0.81 mmol), was suspended in a mixture of EtOH/THF (1:1, 40 mL) and sonicated. NaOH (2 mol L^{-1}, 20 mL) was then added to the solution. After stirring for 5 minutes, the solution turned clear and light brown. The solution was then heated at reflux (80 °C) for 12 h. After cooling, the organic solvents were removed by evaporation, with some white precipitate seen. Additional distilled water (10 mL) was added, and then the solution carefully acidified to pH 4 using HCl (aq, 1 mol L^{-1}) revealing more white precipitate. The solution was then separated using a centrifuge, with the white solid dried on a vacuum filter. Yield 0.65 g, 95%. M.P.: ~330 °C (dec.).

^{1}H NMR (500 MHz, DMSO-d_6): δ = 11.99 *NH* (s, 1H), 8.12 *a* (d, J = 8.1 Hz, 2H), 8.07 *b* (d, J = 8.0 Hz, 2H), 8.02 *c* (d, J = 8.1 Hz, 2H), 7.75 *d* (d, J = 2.0 Hz, 2H), 7.69 *e* (d, J = 8.0 Hz, 2H), 7.49 *f* (d, J = 7.7 Hz, 1H), 7.33 *g* (d, J = 7.7 Hz, 1H), 6.54 *h* (t, J = 2.3 Hz, 1H), 3.81 *i* (s, 6H), 3.20 – 2.90 *a', b', c', d', e'* (m, 22H), 2.75 – 2.73 *f'* (m, 2H), 1.23 – 1.21 *g', h'* (m, 8H), 0.90 *i'* (br s, 2H). Resolvable resonances for COOH were not observed.

^{13}C NMR (125 MHz DMSO-d_6): δ = 167.81, 167.54, 159.94, 155.06, 143.57, 143.23, 142.54, 133.11, 133.01, 130.47, 130.18, 130.00, 129.83, 129.71, 129.46, 129.41, 125.20, 123.60, 121.96, 109.51, 103.56, 70.83, 69.90, 69.74, 69.31, 68.98, 68.79, 56.12, 40.46, 40.30, 40.13, 39.96, 39.79, 39.63, 39.46, 29.43, 25.68.

HR-MS (ToF ES+): Calculated for $[M+H]^+$: $[C_{47}H_{59}N_2O_{12}]^+$ m/z = 845.4100; found m/z = 845.4167.

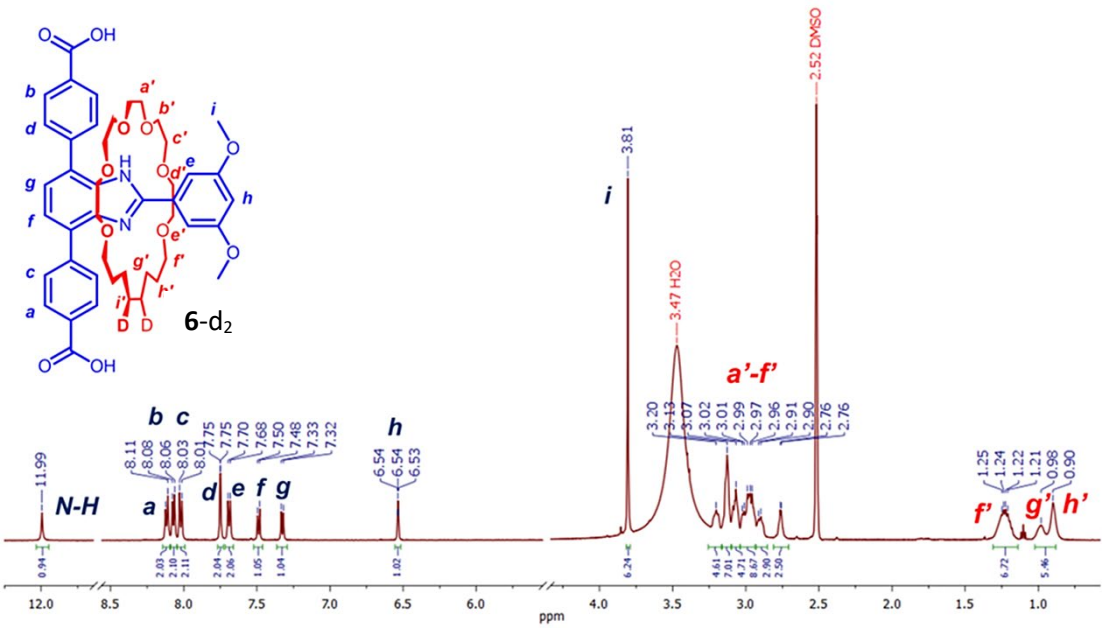

Figure S2. ^{1}H NMR (500 MHz, DMSO-d_6) of compound **6**-d_2, the T-shaped [2]rotaxane linker used to make **UWDM-16**.

Solvothermal Synthesis of UWCM-16

Linker **3** (10.0 mg, 0.020 mmol) was dissolved with in DMF, EtOH and H_2O (3 mL, 3:3:2 v/v) in a screw top 20 mL borosilicate scintillation vial. The solution was sonicated, and $Zn(NO_3)_2.6H_2O$ (15.1 mg, 0.051 mmol) added. The mixture was then sonicated until full solvation and a clear colourless solution was observed. The reaction vial was then placed in a windowed oven at 85 °C for 1 d. After cooling, a white amorphous powder was observed. The powder was filtered off and washed with hot DMF, EtOH and DCM. The recovered powder was weighed. Yield 14 mg, 60%. After drying the powder was found to be crystalline *via* PXRD measurements. Attempts at producing single crystals suitable for SCXRD were not successful.

Solvothermal Synthesis of UWDM-16

Linker **6**-d_2 (10.0 mg, 0.012 mmol) was dissolved with in DMF, EtOH and H_2O (3 mL, 3:3:2 v/v) in a screw top 20 mL borosilicate scintillation vial. The solution was sonicated, and $Zn(NO_3)_2.6H_2O$ (8.8 mg, 0.030 mmol) added. The mixture was then sonicated until full solvation, and a clear colourless solution was observed. The reaction vial was then placed in a windowed oven at 85 °C for 12 h. After 12 h, very large, rhomboid colourless crystals were observed. After cooling, the crystals were filtered off and washed with hot DMF, EtOH and DCM, then placed in anhydrous DCM for further characterisation. The large crystals were suitable for SCXRD directly from the solvothermal synthesis. The remaining crystals were weighed. Yield 13.5 mg, 94%.

3. General Comments on SCXRD Data, PXRD Data, and Topological Analysis

Powder X-ray diffraction data were collected using a capillary mounting goniometer on a Bruker D8 Discover diffractometer equipped with a 140 mm diameter 2-D VÅNTEC-500 detector. CuK_α (λ = 1.54 Å) radiation was used and operated at 40 kV and 40 mA. Variable temperature PXRDs were obtained on the same instrument using an Oxford Cryosystems N_2 700 series Cryostream Cooler.

Single crystal X-ray crystallography diffraction data was collected using a Bruker D8 Venture dual-source diffractometer with a PHOTON 100 detector Kappa goniometer and collected with either CuK_α (λ = 1.54 Å) or MoK_α (λ = 0.71 Å) radiation. Crystals were mounted on MiTeGen Dual-Thickness MicroMounts or MicroLoops and held in place with Hampton Research Parabar 10312. Samples were cooled to 170 K (-103.15 °C) using an Oxford Cryosystems N_2 700 series Cryostream Cooler. Structures were integrated using Bruker APEX5 software and then solved and refined using OlexSys's Olex^2 software.[7]

Topological analysis and net identification of each MOF were made using the GAVROG process using Systre and ToposPro.[8,9] Visualisations of each net and crystal structure were made using the Diamond 3.2k4 software by Crystal Impact.[10] For classification of nets, the resources of the RCSR were used.[11]

SCXRD Structure of 2

Compound **2** was recrystallised from dichloromethane producing colourless rhomboid single crystals. The structure was solved using direct methods and in the triclinic space group, $P\bar{1}$ and included one solvent molecule of CH_2Cl_2. One chlorine atom on the CH_2Cl_2 was modelled for a small degree of positional disorder.

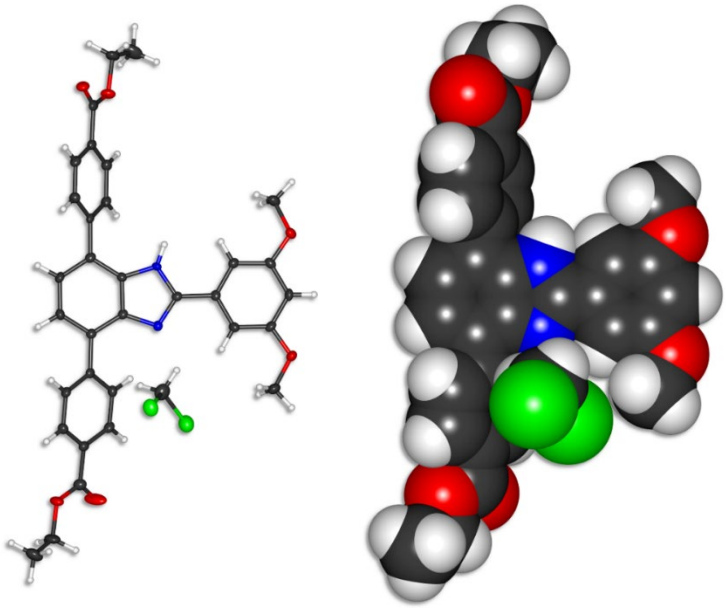

Figure S3. SCXRD structure of **2** displayed as ellipsoids (left) and space-filling (right). Green = Cl, red = O, blue = N, black = C, white = H.

Table S1. Single crystal data, and refinement parameters for **2**.CH_2Cl_2.			
CCDC Number	2500692	Z	2
Formula	$C_{34}H_{32}Cl_2N_2O_6$	ρ_{calc} (g cm^{-3})	1.369
Formula weight (g mol^{-1})	635.55	μ (mm^{-1})	0.260
Crystal system	Triclinic	Reflections used	5431
Space group	$P\bar{1}$	Variables	401
T (K)	135.8	Restraints	0
a (Å)	10.9858(6)	R_1 [I > 2σ (I)][a]	0.0657
b (Å)	11.9858(9)	R_1 (all data)	0.0472
c (Å)	13.2917(7)	wR_2 [I > 2σ (I)][b]	0.1053
α (°)	84.199(2)	wR_2 (all data)	0.1173
β (°)	82.292(2)	GooF on F^2	1.050
γ (°)	62.875(2)	Resolution Range (Å)	6.78 - 0.84
V (Å^3)	1542.02(14)		

[a] $R_1 = \frac{\Sigma||F_o|-|F_c||}{\Sigma|F_o|}$; [b] $R_2w = \sum\left[\frac{\left[w\left(F_{o^2}-F_{c^2}\right)^2\right]}{\Sigma\left[w\left(F_{o^2}\right)^2\right]}\right]^{1/2}$, where $w = q[\sigma^2(F_{o^2}) + (aP)^2 + bP]^{-1}$

SCXRD Structure of 5

Compound **5** produced high-quality crystals from vapour diffusion hexanes into an ethyl ethanoate solution of the compound. The structure was solved using direct methods and in the triclinic space group, $P\bar{1}$. The interlocked macrocyclic ring showed slight disorder between O4R and C7R, but not severe enough for accurate modelling to be required.

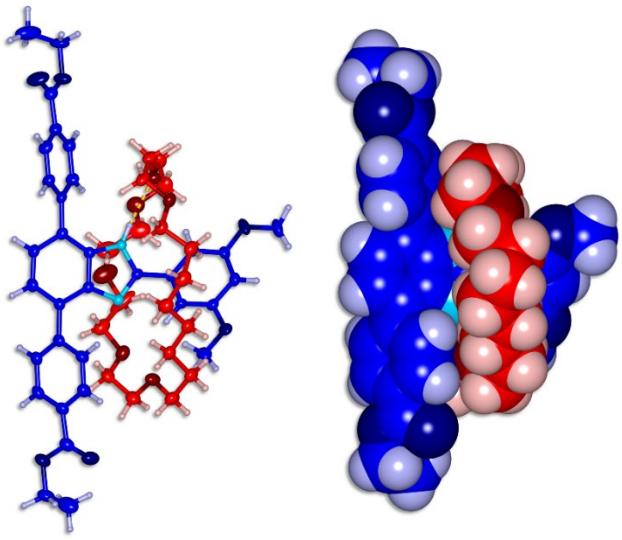

Figure S4. SCXRD structures of **5** displayed as ellipsoids (left) and space-filling (right). Thread: Dark blue = O, light blue = N, blue = C, pale blue = H. Wheel: Dark red = O, red = C, pale red = H.

Table S2. Single crystal data, and refinement parameters for **5**.

CCDC Number	2500693	Z	2
Formula	$C_{51}H_{66}N_2O_{12}$	ρ_{calc} (g cm^{-3})	1.256
Formula weight (g mol^{-1})	899.10	μ (mm^{-1})	0.726
Crystal system	Triclinic	Reflections used	8386
Space group	$P\bar{1}$	Variables	590
T (K)	170.0	Restraints	0
a (Å)	12.1185(3)	R_1 [I > 2σ (I)][a]	0.0587
b (Å)	12.6366(3)	R_1 (all data)	0.1015
c (Å)	16.8865(3)	wR_2 [I > 2σ (I)][b]	0.1142
α (°)	97.8567(14)	wR_2 (all data)	0.1333
β (°)	101.6512(14)	GooF on F^2	1.056
γ (°)	106.4516(14)	Resolution Range (Å)	16.18 - 0.84
V (Å^3)	2376.66(10)		

[a] $R_1 = \frac{\sum||F_o|-|F_c||}{\sum|F_o|}$; [b] $R_2 w = \sum\left[\frac{\left[w\left(F_o{}^2-F_c{}^2\right)^2\right]}{\sum\left[w\left(F_o{}^2\right)^2\right]}\right]^{1/2}$, where $w = q[\sigma^2(F_o{}^2) + (aP)^2 + bP]^{-1}$

SCXRD Structure of UWDM-16

Colourless rhomboid crystals were produced from the solvothermal synthesis shown in Figure S7. The crystals showed weak diffraction, and the data was treated as a merohedral twin. Modelling of the macrocycle required several DFIX and DANG restraints, but the framework connectivity is well resolved.

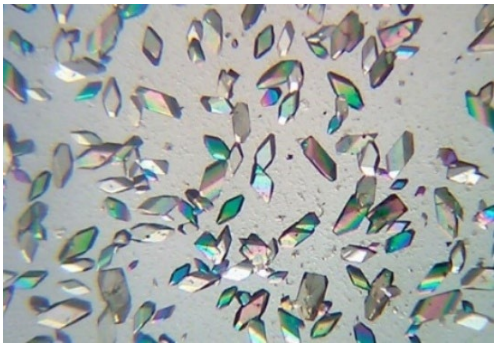

Figure S5. Microscope Image of **UWDM-16**[As-Synth] crystals.

Table S3. Single crystal data, and refinement parameters for **UWDM-16**			
CCDC Number	2500694	Z	3
Formula	$C_{282}H_{342}N_{12}O_{75}Zn_6$	ρ_{calc} (g cm^{-3})	1.053
Formula weight (g mol^{-1})	5491.88	μ (mm^{-1})	1.018
Crystal system	trigonal	Reflections used	6419
Space group	$R\bar{3}$	Variables	553
T (K)	170.0	Restraints	252
a (Å)	25.8311(5)	R_1 [I > 2σ (I)][a]	0.1224
b (Å)	25.8311(5)	R_1 (all data)	0.1257
c (Å)	44.9688(14)	wR_2 [I > 2σ (I)][b]	0.3411
α (°)	90	wR_2 (all data)	0.3494
β (°)	90	GooF on F^2	1.774
γ (°)	120	Resolution Range (Å)	20.00 - 0.98
V (Å^3)	25985.3(13)		

[a] $R_1 = \frac{\sum||F_o|-|F_c||}{\sum|F_o|}$; [b] $R_2 w = \sum\left[\frac{\left[w\left(F_{o^2}-F_{c^2}\right)^2\right]}{\sum\left[w\left(F_{o^2}\right)^2\right]}\right]^{1/2}$, where $w = q[\sigma^2(F_{o^2}) + (aP)^2 + bP]^{-1}$

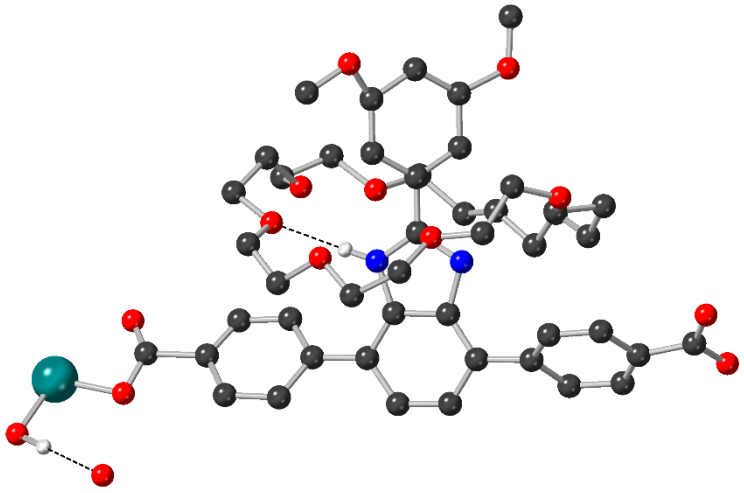

Figure S6. A ball-and-stick representation of the SCXRD structure of **UWDM-16** showing the contents of the asymmetric unit. Teal = Zn(II) , red = O, blue = N, black = C, white = H. Only the H-atoms involved in hydrogen bonding are shown for clarity

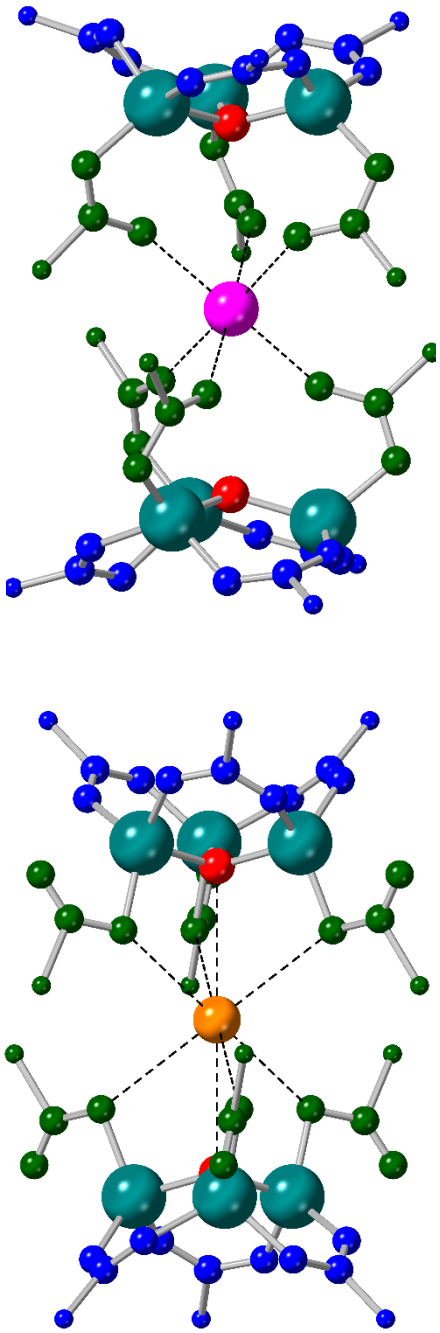

Figure S7. Top: the (12)-c heptanuclear, $[Zn_6(\mu_3\text{-}OH)_2(O_2C\text{-})_{12}Na]$ SBU reported by Ng *et al*.[12] Bottom: the (12)-c hexanuclear $[Zn_6(\mu_3\text{-}OH)_2(\mu_2\text{-}RCO_2)_6(\eta^1\text{-}RCO_2)_2(\eta^1\text{-}RCO_2H)_4(\mu\text{-}H_2O)]$ SBU found by SCXRD for **UWDM-16**.

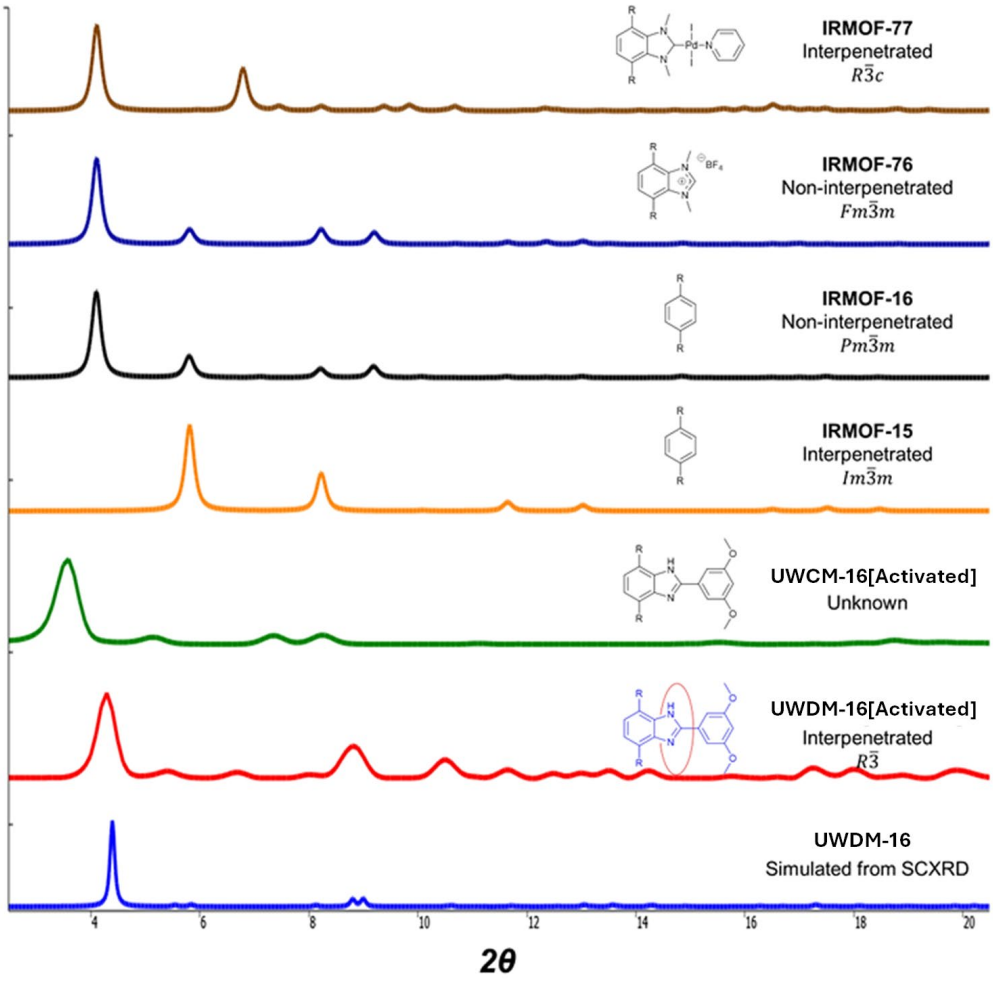

Figure S8 Comparison of PXRDs of **UWCM-16** and **UWDM-16** with MOFs in Yaghi's IRMOF series of ditopic triphenyl dicarboxylate Zn MOFs. All MOFs are **pcu**.[13,14]

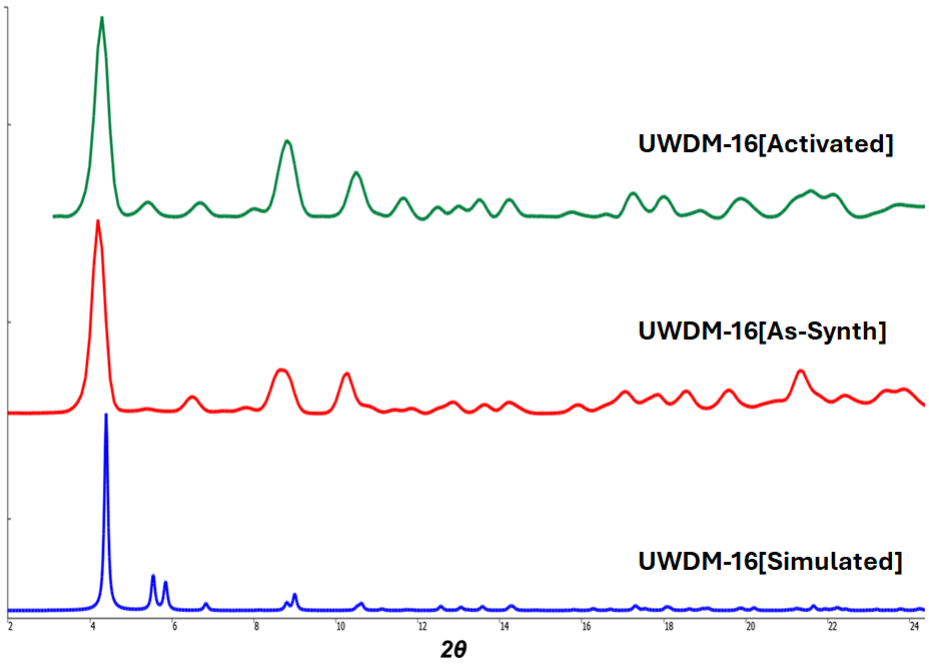

Figure S9. Powder X-Ray Diffraction of **UWDM-16**. Blue: Simulated from SCXRD CIF. Red: As-synthesised MORF. Green: Activated MORF.

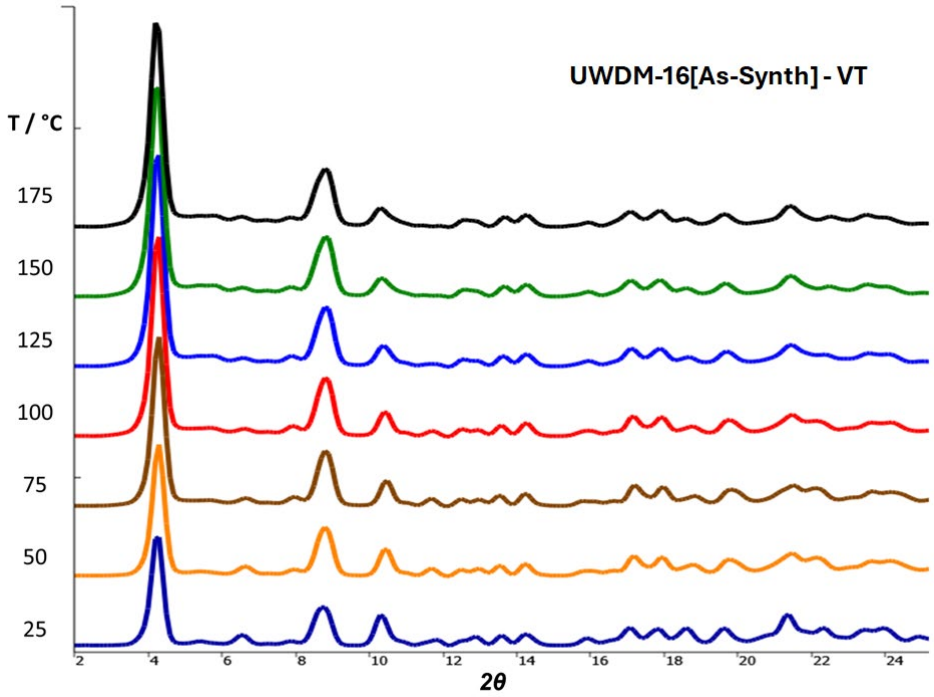

Figure S10. Variable Temperature Powder X-Ray Diffraction of **UWDM-16**[As-Synth].

4. Variable Temperature Deuterium (^{2}H) Solid-State NMR of UWDM-16

^{2}H SSNMR experiments were performed on a Bruker Avance III HD console equipped with an Oxford 9.4 T magnet with Larmor frequencies: $\nu_0(^1H)$ = 399.73 MHz and $\nu_0(^2H)$ = 61.4 MHz. A Chemagnetics 4 mm double resonance (HX) MAS probe was used for all experiments. The quadrupolar-echo pulse sequence (90° – τ_1 – 90° – τ_2 – acquire) was used with recycle delays between 0.5 and 1.0 s recycle delays, 2.5 µs optimized 90° pulses, and 50 µs interpulse spacings. High-power ^{1}H decoupling fields of 50 kHz were used in all experiments. Temperatures of the VT unit and probe were calibrated using the temperature-dependent chemical shift of $Pb(NO_3)_2$.[15] The quadrupolar parameters of the slow-motion limit (SML) spectrum was determined using the Solid Lineshape Analysis (SOLA) module in TopSpin 3.5. Simulations of the intermediate-motion regime (IMR) and fast-motion limit (FML) spectra were conducted using EXPRESS.[16]

^{2}H SSNMR Analysis of the Dynamics of the Mechanically Bound Wheel

Variable-temperature (VT) ^{2}H SSNMR experiments were conducted for this sample at temperatures ranging from 173 K to 448 K in 25 K increments (Fig. S12). At the lowest temperatures, powder patterns with sharp discontinuities are observed. Despite the presence of interference on the lower frequency side of the spectrum, the pattern is symmetric and can be simulated using values of C_Q = 158(3) kHz and η_Q = 0.05(5). The pattern at 173 K indicates ^{2}H sites undergoing motion in the SML, with rates < 1 kHz. As the temperature increases, the sharp, outer features of the pattern persist, while there is a buildup of signal in the centre of the pattern indicative of a two-site jump motion with β = 77°; at 223 K, this occurs at a rate of *ca*. 10 kHz. The rate of this 77° two-site jump enters the fast motion limit (*i.e.,* the point where faster motions cease to have an effect on the NMR spectrum line shape) at 323 K. Starting at 373 K, simulation of the pattern requires the consideration of partial rotation; Table S4 details the rates of both the two-site jump and partial rotation at select temperatures based on a preliminary set of simulations. Both the modes of motion have been observed in analogous MOFs, with the onset of two-site jumps always occurring at lower temperatures than those of the partial rotations.[6,11,12] However, based on simulations, the specific onset temperatures for these motions occur at higher temperatures relative to those of our original dynamic MOF, **UWDM-1**.[11] For this sample, FML two-site jump motion is achieved at 323 K, which is *ca.* 75 K higher than for **UWDM-1**.[11] By 323 K, partial rotation is detectable in **UWDM-1**, while there is no evidence of partial rotation in **UWDM-16** until 373 K. Finally, in contrast to **UWDM-1**, there is no evidence of full rotation in **UWDM-16** at any temperature.

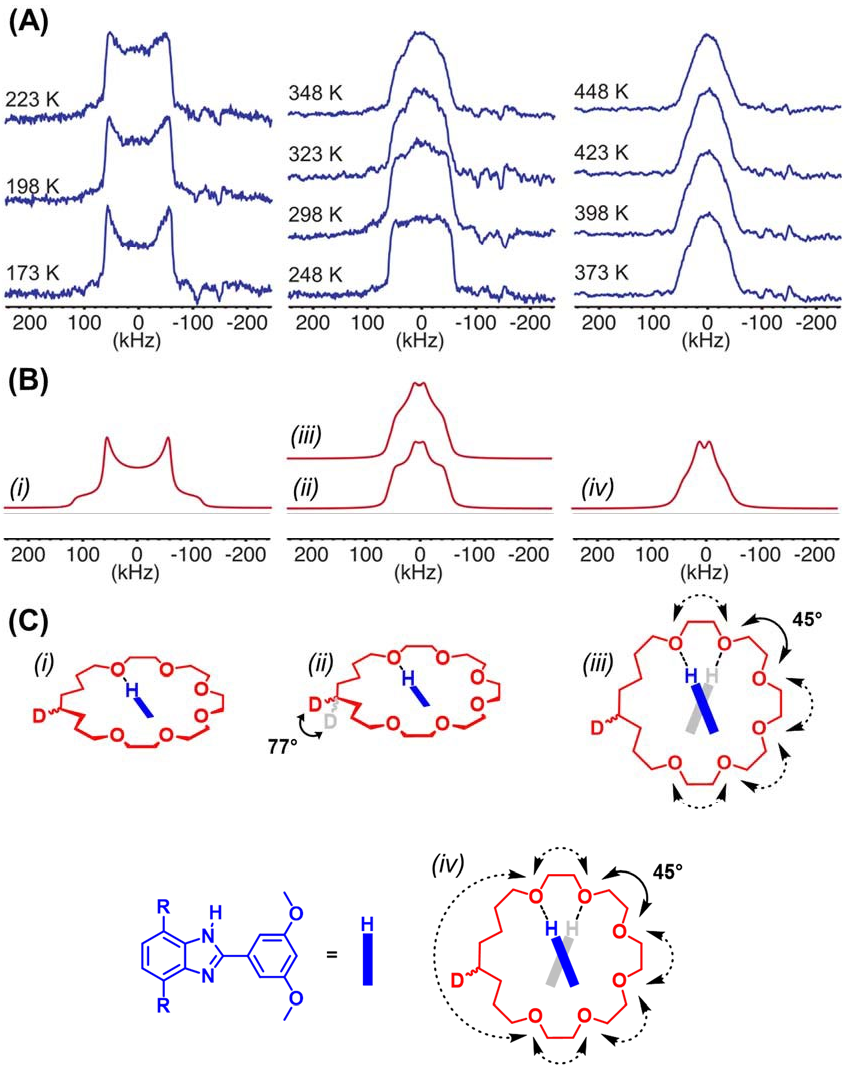

Figure S11. (A) Experimental VT ^{2}H SSNMR powder patterns for **UWDM-16 [Activated]**. (B) Simulated ^{2}H SSNMR powder patterns for the (i) motions that are too slow to influence the appearance of the Pake doublet (i.e., in the SML), (ii) a two-site jump motion in the fast motion limit (FML, $v_{ex} > 10^{6}$ Hz) (iii) FML two-site jumps and 1 kHz partial rotation of the ring over 225° in 45° steps, and (iv) FML two-site jumps and 20 kHz partial rotation. (C) The four possible modes of rotation around the benzimidazole axle. (i) Immobile, or at the SML between 173-223 K. (ii) The two-site jump in the FML between 248-348 K. (iii) Partial rotation between 373-448 K. (iv) Full rotation including the alkyl chain is not observed in **UWDM-16**.

Table S4. Modes and rates of motion used in the simulations of select experimental VT ^{2}H SSNMR spectra for **UWDM-16**.

Temperature (K)	Two-Site Jump (Hz)	Partial Rotation (kHz)
173	< 1	0
223	10(5)	0
298	10000(5000)	0
323	>1000000	0
373	>1000000	1(1)
448	>1000000	100(20)

Uncertainties in the last digits are indicated in parentheses (e.g., 10000(5000) = 10000 ± 5000

4. References

1. A. F. Kilbinger, S. J. Cantrill, A. W. Waltman, M. W. Day, R. H. Grubbs, *Angew. Chem. Int. Ed.*, 2003, **42**, 3281-3285.
2. K. Pilgram, M. Zupan, R. Skiles, *J. Heter. Chem.* 1970, **7**, 629-633.
3. G. Baggi, S. J. Loeb, *Angew. Chem.*, 2016, **128**, 12721-12725.
4. B. A. Neto, A. A. Lapis, E. N. da Silva Júnior, J. Dupont, *Eur. J. Org. Chem.*, 2013, **2013**, 228-255.
5. B. A. D. Neto, A. S. Lopes, M. Wüst, V. E. Costa, G. Ebeling, J. Dupont, *Tet. Lett.* 2005, **46**, 6843-6846.
6. Z.-H. Zhang, L. Yin and Y.-M. Wang, *Cat. Comm.*, 2007, **8**, 1126-1131.
7. O. V. Dlomanov, L. J. Bourhis, R. J. Gildea, J. A. Howard, H. Puschmann, *J. App. Cryst.* 2009, **42**, 339-341.
8. V. A. Blatov, A. P. Shevchenko, D. M. Proserpio, Cryst. Grow. Des., 2014, 14, 3576-3586.
9. S. Barthel, E. V. Alexandrov, D. M. Proserpio, B. Smit, *Cryst. Growth Des.*, 2018, **18**, 1738-1747.
10. W. T. Pennington, *J. App. Cryst.*, 1999, **32**, 1028-1029.
11. M. O'Keeffe, M. A. Peskov, S. J. Ramsden, O. M. Yaghi, *Acc. Chem. Res.*, 2008, **41**, 1782-1789.
12. L. Hou, J. P. Zhang, X. M. Chen, S. W. Ng, *Chem. Commun.*, 2008, 4019-4021.
13. M. Eddaoudi, J. Kim, N. Rosi, D. Vodak, J. Wachter, M. O'Keeffe and O. M. Yaghi, *Science*, 2002, **295**, 469-472.
14. C. Li, W. Qiu, W. Shi, H. Song, G. Bai, H. He, J. Li, M. J. Zaworotko, *CrystEngComm*, 2012, **14**, 1929-1932.
15. T. Takahashi, H. Kawashima, H. Sugisawa, B. Toshihide, *Solid State Nucl. Magn. Reson*. 1999, **15**, 119–123.
16. R. L. Vold and G. L. Hoatson, *J. Mag. Res.*, 2009, **198**, 57–72.